JOURNAL OF GEOPHYSICAL RESEARCH, VOL. 113, D15124, doi:10.1029/2007JD009676, 2008

Comparison of atmospheric hydrology over convective continental regions using water vapor isotope measurements from space

Derek Brown,[1] John Worden,[2] and David Noone[1]

Received 5 December 2007; revised 27 May 2008; accepted 6 June 2008; published 15 August 2008.

[1] Global measurements of the 500–825 hPa layer mean HDO/H_2O ratio from the Tropospheric Emission Spectrometer (TES) are used to expose differences in the dominant hydrologic processes in the Amazon, north Australian, and Asian monsoon regions. The data show high regional isotopic variability and numerous values unexpected from classical Rayleigh theory. Correlation analysis shows that mixing with boundary layer air, enhanced isotopic fractionation during precipitation, and subsiding air parcels contribute to intraseasonal isotopic variability. These local controls explain only 8–30% of total regional variance, which suggests that the isotopes are primarily indicators of moist processes that occur upstream. Seasonal trajectory analysis demonstrates that Rayleigh distillation in a Lagrangrian framework underestimates the observed isotopic depletion during the monsoons and suggests substantial recycling of water within or below clouds. The trajectory results for the dry seasons reveal that subsiding air parcels periodically introduce isotopically depleted air into the north Australia and Asian monsoon regions, whereas vigorous low-level convection over the Amazon basin acts to quickly enrich and moisten dry subsiding air. The analysis indicates variations in the strength of convective detrainment into the lower to middle troposphere over all regions, which, during the dry seasons of the north Australian and Asian monsoon regions, correlate with increases in relative humidity. This study shows that isotopic measurements provide unique diagnostics of mechanisms that control the seasonal sources of water and that these provide a refined understanding of the differences in the characteristics of hydrologic budgets in these monsoonal regions.

Citation: Brown, D., J. Worden, and D. Noone (2008), Comparison of atmospheric hydrology over convective continental regions using water vapor isotope measurements from space, *J. Geophys. Res.*, *113*, D15124, doi:10.1029/2007JD009676.

1. Introduction

[2] The hydrologic regimes of the monsoonal regions of Southeast Asia, South America and northern Australia reflect a complex balance of large-scale advective supply of water, surface exchange, and atmospheric condensation, which are important for the regional energy balance and climate [*Malhi et al.*, 2002; *Martinelli et al.*, 1996; *Sengupta and Sarkar*, 2006; *Fu and Li*, 2004; *Juárez et al.*, 2007; *Salati and Vose*, 1984; *Tian et al.*, 2007]. For these regions, the transfers of heat and moisture from the land surface to the atmosphere are substantial, yet these mechanisms are poorly resolved in current land-atmosphere models [*Dirmeyer et al.*, 2006]. There is a need to further understand the seasonal variations in the sources of moisture over monsoonal regions to better constrain the surface water budget, identify the fate of precipitation, and establish the relationship between runoff, evapotranspiration, and the recycling of rainfall by cloud processes [*Henderson-Sellers et al.*, 2004; *McGuffie and Henderson-Sellers*, 2004].

[3] Measurements of water isotopes are useful for analyzing the sources and history of moisture because the lighter isotopes of water (e.g., H_2O) preferentially evaporate over heavier isotopes of water (e.g., HDO or $H_2^{18}O$), and heavier isotopes preferentially condense. Furthermore, the isotopic composition of ocean waters, and hence the vapor immediately evaporated from the ocean is well known; consequently, comparison of measured isotopic values of moisture with respect to oceanic values can be used to identify fresh vapor versus vapor that has a history of condensation. For example, *Dansgaard* [1964] and *Gat* [1996] showed that as oceanic air is advected away from the primary moisture source, isotopic fractionation during condensation causes precipitation to become depleted with respect to the deuterium content. This mechanism (hereafter Rayleigh model) leads to stronger isotopic depletion with higher latitude, altitude, and distance from coast. This model has been successful in explaining high-latitude precipitation and also has provided useful insight into prior climatic temperature variations [*Fricke and Wing*, 2004; *Jouzel et al.*, 2003; *Blunier et al.*, 2004; *Dansgaard*, 1964].

[1] Department of Atmospheric and Oceanic Sciences and Cooperative Institute for Research in Environmental Sciences, University of Colorado, Boulder, Colorado, USA.
[2] Jet Propulsion Laboratory, California Institute of Technology, Pasadena, California, USA.

0148-0227/08/2007JD009676$09.00

However, it is not clear if the Rayleigh model is generally appropriate for studies using high-frequency (event-based) measurements, nor is it clear if the model is appropriate for explaining the isotopic composition of tropical vapor and precipitation over monsoonal regions.

[4] Over monsoonal regions, precipitation rates and monsoonal circulation patterns are thought to be the dominant controls on the seasonal isotopic composition of water vapor and rainfall [*Hoffmann*, 2003]. For example, using the International Atomic Energy Agency Global Network for Isotopes in Precipitation data set (GNIP), *Vimeux et al.* [2005] found no correlation between the isotopic composition of Amazonian rainfall and local temperature values, but instead correlations between the rainfall's isotopic composition and upstream condensation rates. Additionally, *Vuille et al.* [2005] found a significant negative relationship between ^{18}O abundance in precipitation and the strength of the Asian monsoon, indicating a connection between increased precipitation rates and isotopic depletion. This connection is known as the "amount effect", which is a term used to describe isotopic depletion during rainfall that is beyond that predicted by Rayleigh distillation. The amount effect is important in all areas experiencing significant monsoonal flows [*Dansgaard*, 1964; *Rozanski et al.*, 1992; *Rozanski and Araguas-Araguas*, 1995; *Araguas-Araguas et al.*, 1998], and has been documented using isotopic signals in precipitation, including ice and snow in both the Himalaya [*Wushiki*, 1977] and the Andes [*Grootes et al.*, 1989]. However, different mechanisms have been used to explain the amount effect and it is likely that multiple effects are responsible. For example, *Dansgaard* [1964] and *Rozanski et al.* [1993] explained that the amount effect of tropical precipitation is primarily due to the high fractional removal of heavy isotopes during intense condensation at high altitudes; they also suggested that reevaporation of raindrops below the cloud base leads to a high relative loss of heavy isotopes in arid conditions.

[5] Variations in the isotopic composition reflect the history of moist processes for each observed air parcel, which can be used to determine the strength of the contributing processes. Hereafter, the abundance of singly deuterated water relative to common water is expressed in terms of a "delta" value:

$$\delta D = \left[\frac{(HDO/H_2O)_{obs}}{(HDO/H_2O)_{VSMOW}} - 1 \right] \times 1000 \qquad (1)$$

where HDO and H_2O are proportional to the number of molecules of each species. The ratio $(HDO/H_2O)_{VSMOW}$ is the Vienna Standard Mean Ocean Water standard and is 311.52×10^{-6}. With this definition, one simple description of the effects of condensation on atmospheric water vapor can be given as a Rayleigh distillation. The Rayleigh model for condensation, as introduced by *Dansgaard* [1964], predicts for the isotopic composition of atmospheric water vapor after condensation, and is given by

$$\frac{\delta D}{1000} = \left(\frac{\delta D_O}{1000} + 1 \right) \cdot F^{(\alpha - 1)} - 1 \qquad (2)$$

where F is the fraction of initial moisture remaining in the given air mass, α is the effective fractionation factor during formation of raindrops and/or ice crystals at the cloud temperature, and δD_0 is the initial delta value of the vapor. This model describes the increased isotopic depletion as water vapor is continuously removed via condensation.

[6] While the Rayleigh model is useful in illustrating some bulk features of atmospheric isotope hydrology and indeed models the isotopic depletion of simple large-scale condensation events credibly, there are processes not included that limit its application for studies of the isotopic balance of water vapor. The effects of air mass mixing, reevaporation of precipitation, and isotopic exchange of vapor with precipitation act to introduce isotopic variability of the residual vapor beyond that predicted by the simple Rayleigh model [*Webster and Heymsfield*, 2003; *Lawrence et al.*, 2004; *Schmidt et al.*, 2005; *Worden et al.*, 2007]. Moreover, regional and local effects involving evapotranspiration, turbulent transport, precipitation rates, and ice lofting are thought to further modify the isotopic composition of atmospheric water vapor, leading to distinct regional differences in isotopic composition [e.g., *McGuffie and Henderson-Sellers*, 2004; *Hoffmann*, 2003; *Araguas-Araguas et al.*, 2000]. For example, the continental gradient in the stable water isotope composition of rainfall is very weak for the Amazon region, and suggests strong local water recycling and the influence of transpiration [*Henderson-Sellers et al.*, 2002]. These studies show that a more detailed explanation of the regional hydrology emerges by considering not only the isotopic composition itself, but the degree to which isotopic observations deviate from that predicted by simple expectations (such as that from a Rayleigh model).

[7] The purpose of the present study is to explain the seasonal variation of the hydrologic regime over three tropical continental areas (the Amazon, north Australia, and Asian monsoon regions) in which seasonal monsoon circulations dominate. Of particular interest is providing an assessment of the contributions from advection, local and upstream convection, in situ condensation, recycling of vapor within regions of organized convection, and evapotranspiration. The analysis makes use of the near-global lower to middle troposphere HDO/H_2O ratio data from the Tropospheric Emission Spectrometer (TES) [*Worden et al.*, 2006]. With this data, analyzing isotopic exchange during turbulent mixing and intense condensation exposes the limitations of simple explanations based on Rayleigh distillation. In order to enable interpretation of the regional hydrology from isotopes, the meteorological processes which control the isotopic composition must first be established. By examining and contrasting the hydrologic budget inferred from the isotope measurements with budgets computed from nonisotope methods, insight is gained into those hydrological processes that are common to and those that are different between the three tropical continental regions.

2. Annual and Seasonal Distribution of TES δD

[8] The HDO/H_2O data from TES on NASA's Aura spacecraft offers a unique global-scale view of the isotopic composition of water vapor. TES is a Fourier transform spectrometer that measures the infrared energy emitted by Earth's surface and by gases and particles in Earth's atmosphere. TES has high spectral resolutions of 0.025 cm^{-1} in

limb mode and 0.1 cm^{-1} in nadir mode, which gives it the ability to resolve the shape of individual emission lines. Data used for this study comes from TES's nadir mode, which observes a horizontal area of approximately 5.3 km × 8.3 km. Accurate estimation of the isotope ratio results from a joint retrieval algorithm that allows partial cancellation of systematic errors common to both HDO and H_2O [*Worden et al.*, 2006]. Additional selection of the data is required to ensure only high-quality and physically meaningful retrievals are used [*Worden et al.*, 2007]. TES data used in this study comes from 249 days from August 2004 to December 2006. Two seasonal data sets are created from data retrievals from December to February (DJF) and June to August (JJA) dates, respectively. The DJF data contain 78 days; 39 days from 2004 to 2005, 25 days from 2005 to 2006, and 14 days from 2006. The JJA data contain 55 days; 2 days from 2004, 17 days from 2005, and 34 days from 2006. Aura orbits sixteen times each day while recovering approximately 500–3000 high-quality profiles of atmospheric δD. A reduction of 5% on the volume mixing ratio of HDO has been used in this study to calculate the final δD values in order to account for an unknown bias in the spectroscopic line strengths [*Worden et al.*, 2007]. The TES retrieval has typically around 1 degree of freedom in the vertical with an error of ±10‰ on calculated δD values [*Worden et al.*, 2006], and the retrieval is most sensitive to a thick layer in the lower troposphere. As such, we restrict our analysis to lower troposphere mean values.

[9] The annual, mass-weighted average values over the layer 500–825 hPa for temperature, specific humidity, and δD from TES are shown in Figure 1. Figure 1a shows a poleward decrease in annual temperature with weak longitudinal variations along the equator, while Figure 1b indicates that tropical continental areas and the Pacific warm pool contain the greatest amounts of water vapor in the 500–825 hPa layer average. The highest specific humidity values also coincide with areas known to experience frequent and intense convection (e.g., the Pacific Warm Pool), which suggests that water vapor is being moved vertically into the 500–825 hPa column from below. The TES annual δD values (Figure 1c) show detail of the isotopic effects of convection and condensation. The general poleward decrease in annual δD values reflects continual isotopic depletion occurring as water moves poleward, cools, and condenses. In the tropics, *Worden et al.* [2007] suggest that higher δD values are indicative of water vapor, which has been exposed to evaporation from the ocean and is therefore isotopically "heavy", being lofted into the 500–825 hPa layer from below. However, Figure 1c shows that areas known to have the strongest convection in the annual mean (i.e., the Amazon and the Pacific warm pool), do not necessarily have the highest δD values in the annual mean. This may suggest that in the areas of strongest convection, isotopic depletion by intense condensation offsets the enrichment from surface evaporation. In order to expose the underlying causes of these differences, the regional balances between advection, moist convection, condensation, and the isotopic composition of atmospheric waters must be established.

[10] Figure 2 shows seasonal differences, defined as the December–February (DJF) average minus the June–August (JJA) average, in temperature, specific humidity, and δD. The DJF-JJA temperature differences (Figure 2a) maintain zonal symmetry outside the tropics, while asymmetry arises in the equatorial regions because of the seasonal shift in the atmospheric convergence zones and differences in the land-sea temperature contrasts. What emerges in Figure 2b is a strong hemispheric symmetry with more water vapor over continents during the monsoonal wet seasons with evidence of downstream advection to nearby oceanic areas. The seasonal differences in δD (Figure 2c) show that the Amazon and north Australian regions, where strong monsoonal rains characterize the regional climate, have large seasonal variation in the isotopic composition. A significant seasonal difference in mean δD values is not seen over the Asian monsoon region. Further, the seasonal differences in δD over north Australia and the Amazon basin are of opposite sign, even though these regions are at similar latitudes and both experience monsoonal type flow in the same season. Specifically, vapor over the rain forests of the Amazon is more depleted in deuterium during this region's wet season (DJF) than during the dry season (JJA), where as the opposite is true for the more arid north Australian region. These δD anomalies over different land surfaces with well-defined monsoonal seasons immediately suggest differences in the balance of processes contributing to the hydrological balance in each region.

3. Local Controls on Isotopic Composition

[11] To establish the importance of local processes relative to large-scale influences (specifically advection), the relationship between the measured isotopic composition and meteorological parameters that capture the strength of the local processes are examined. Of interest are the associations between δD values and local temperature, specific humidity, relative humidity, precipitation rate, lapse rate, and large-scale horizontal moisture flux. These relationships indicate the importance of condensation, entrainment of recently evaporated air, and large-scale advection. Each quantity is derived from the TES observations as 500–825 hPa layer mean values, with two exceptions. First, precipitation rates are taken from the Global Precipitation Climatology Project (GPCP) daily average rainfall rates and spatially interpolated to the locations of the TES observations. Second, the scalar moisture flux values were found by integrating the product of TES specific humidity and spatially interpolated NCEP horizontal wind speeds over the five TES vertical levels between 500 and 825 hPa. The predictors described above are used for standardized linear and multiple regressions against TES δD values in Tables 1 and 2, respectively. For the analysis the Amazon is defined to be within the box bounded between 0–20°S and 290–310°E, north Australia as between 10–22.5°S and 120–140°E, and the Asian monsoon region as between 15–30°N and 80–100°E. These definitions are mostly continental, although in the case of the north Australian and the Asian monsoon regions, some oceanic area is included. All individual, and instantaneous, TES observations falling within these regions are used in the analysis. There are approximately equal numbers of daytime and nighttime observations for each region and season.

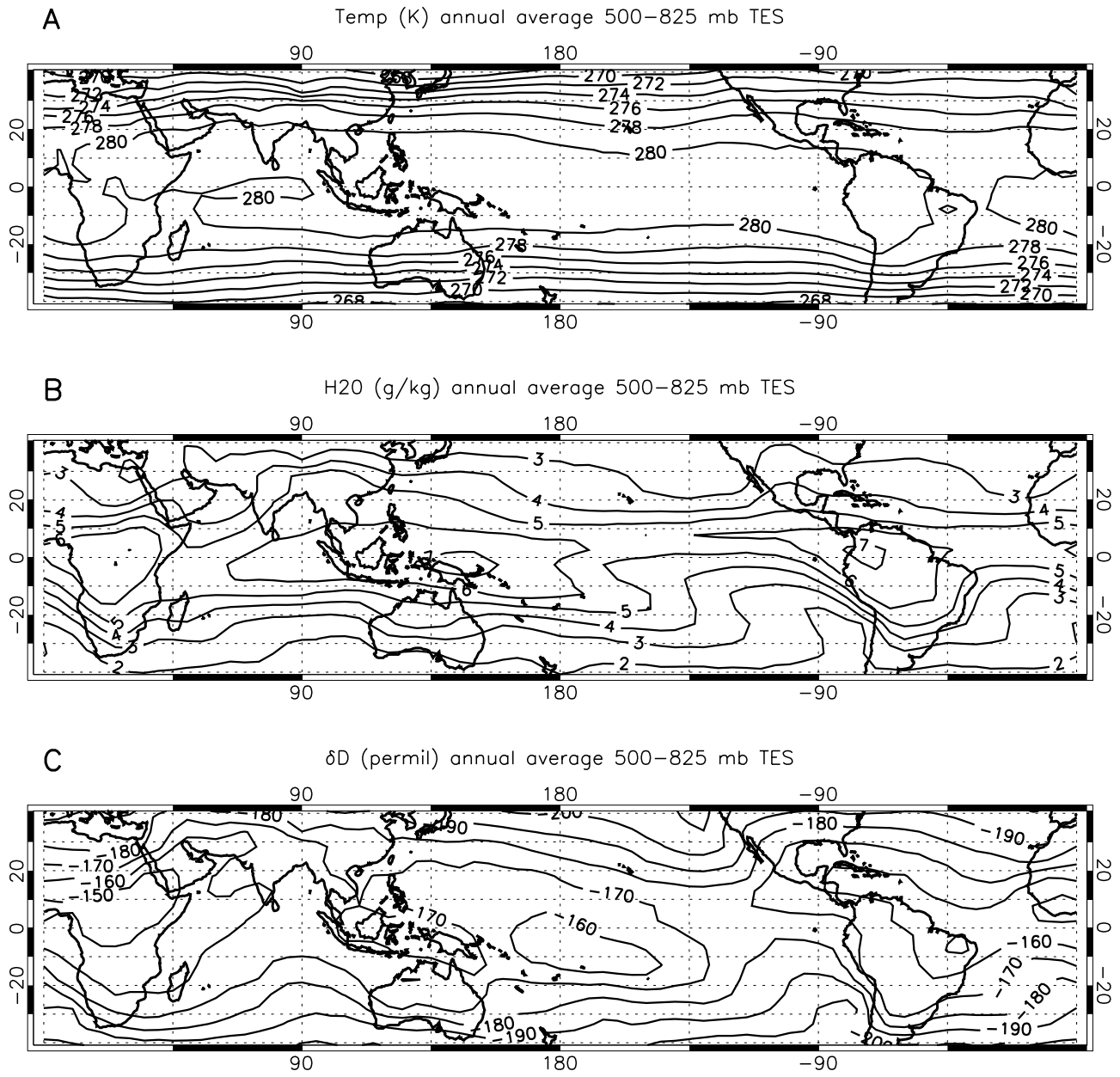

Figure 1. TES annual average (a) temperature, (b) specific humidity, and (c) δD for the layer 500–825 hPa over August 2004 to December 2006. Contour intervals are 2 K (Figure 1a), 1 g/kg (Figure 1b), and 10 ‰ (Figure 1c).

3.1. Rayleigh Perspective in Monsoon Regions

[12] Variations in water isotope composition are often considered to be simply associated with temperature. For vapor undergoing continual condensation, Rayleigh distillation predicts that δD values should decrease as air parcels cool because of condensation, yet no positive linear or partial correlations are found between δD and temperature for any season over the monsoon regions (Tables 1 and 2, respectively). This result largely agrees with results based on precipitation isotope data that show strong positive temperature correlations in monthly data outside the tropics and almost no correlation in warmer areas [e.g., *Dansgaard*, 1964]. Moreover, contrary to Rayleigh theory, the linear regression coefficients in Table 1 are significant and negative between δD and temperature during the dry seasons of the Asian monsoon (−0.35) and north Australian (−0.12) regions (explored in detail in sections 3.2 and 3.3 below). In order to better explain these variations in the isotopic composition of monsoon vapor, additional models must be added to Rayleigh distillation.

[13] Figure 3 shows δD values within each region presented as a function of specific humidity for their respective wet and dry seasons. The wet season for the Amazon and north Australian regions is shown for the DJF time period and for the Asian monsoon region in the JJA time period. Rayleigh distillation lines originating from air parcels with saturation specific humidity values based on oceanic temperatures of 285 K and 300 K, and initial δD values of

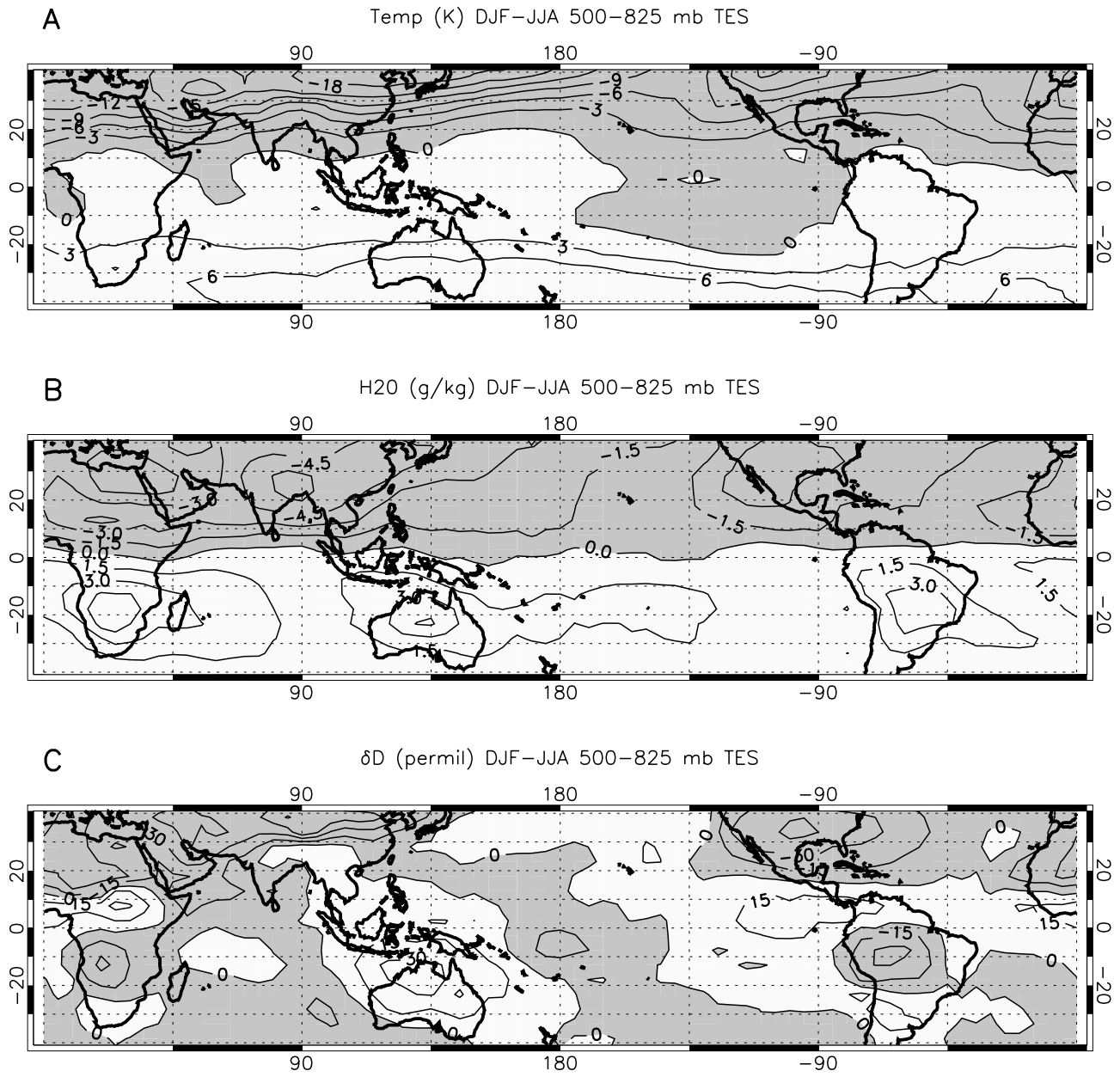

Figure 2. TES DJF-JJA difference in (a) temperature, (b) specific humidity, and (c) δD for the layer 500–825 hPa over August 2004 to December 2006. Grey shading indicates negative values, and contour intervals are 3 K (Figure 2a), 1.5 g/kg (Figure 2b), and 15 ‰ (Figure 2c).

−79‰ (approximately that of vapor in equilibrium with the ocean), are shown as black lines. Grey lines representing the enriching effects that mixing relatively moist marine and transpired air with drier air parcels are also shown, and are based on a typical tropical surface temperature of 292 K. A model for this enriching effect is described in the supplemental material of *Worden et al.* [2007].

[14] Most data are more depleted than both evaporation lines, suggesting that most observations have a history of condensation. The regional dry season data (Figures 3a, 3c, and 3f) are reasonably constrained by the Rayleigh distillation and marine evaporation lines, while the wet season data (Figures 3b, 3d, and 3e) show many δD values that are more depleted than predicted by Rayleigh distillation. These wet

Table 1. Standardized Linear Regressions of TES δD With Lapse Rate, Relative Humidity, Precipitation, Scalar Moisture Flux, Temperature, and Specific Humidity[a]

Region	Season	Γ	RH	*P*	*V*·*q*	*T*	*q*
Amazon	*JJA*	**−0.24**	**−0.13**	−0.02	−0.04	0.07	−0.05
Amazon	*DJF*	**−0.15**	**−0.39**	**−0.21**	**0.10**	0.02	**−0.34**
North Australia	*JJA*	**−0.28**	**0.16**	0.00	0.02	**−0.12**	**0.17**
North Australia	*DJF*	**−0.32**	**−0.34**	**−0.27**	**−0.26**	−0.10	**−0.35**
Asian monsoon	*JJA*	−0.06	**−0.32**	**−0.16**	**−0.16**	−0.03	**−0.28**
Asian monsoon	*DJF*	**−0.21**	**0.28**	−0.08	**0.27**	**−0.35**	**0.26**

[a]Significance levels over 95%, as determined by Student's *t* test, are indicated in bold. Γ, lapse rate; RH, relative humidity; *P*, precipitation; *V*·*q*, scalar moisture flux; *T*, temperature; and *q*, specific humidity.

Table 2. Multiple Correlation Coefficients and Beta Weights for a Standardized Multiple Regression of δD Versus Five Predictors[a]

Region	Season	$100*R^2$	Γ	RH	P	$V{\cdot}q$	T
Amazon	JJA	**08**	**−0.26 (02)**	**−0.14 (07)**	0.06 (08)	0.01 (08)	0.07 (08)
Amazon	DJF	**30**	−0.09 (29)	**−0.62 (09)**	**−0.17 (27)**	**0.20 (26)**	**−0.28 (26)**
North Australia	JJA	**10**	**−0.24 (05)**	**0.20 (09)**	−0.01 (10)	**−0.19 (09)**	−0.06 (10)
North Australia	DJF	**26**	**−0.28 (20)**	**−0.32 (20)**	−0.11 (25)	−0.09 (25)	−0.09 (25)
Asian monsoon	JJA	**14**	0.03 (14)	**−0.37 (04)**	−0.07 (14)	−0.03 (14)	**−0.19 (12)**
Asian monsoon	DJF	**20**	−0.11 (19)	0.00 (20)	−0.09 (19)	**0.24 (18)**	**−0.29 (15)**

[a]Correlation coefficients are squared and shown in percentage (column 3). Beta weights are defined as the standardized regression coefficients (columns 4–8). Specific humidity (q) has been eliminated from the regression model because of strong correlations between q and RH across all regions and seasons. Values in parentheses represent the variance in δD explained using a multiple regression model that excludes the respective predictor. Bold values indicate significance at the 95% level, based on the partial correlations of the respective variables.

season values may be explained by substantial isotopic exchange occurring during heavy rainfall [e.g., *Rozanski et al.*, 1993] or by evaporation of falling raindrops [e.g., *Worden et al.*, 2007]. However, the large variance in δD values for all regions suggests mixing processes, including turbulent transport and large-scale advection, plays a crucial role in the local isotopic variance. Additionally, the Amazon (Figures 3a and 3b) and north Australia observations (Figure 3d), where the δD values exceed the δD values of evaporated oceanic water, are likely signals of transpired water since they can be explained by a source with an isotopic composition similar to precipitation in the respective regions.

3.2. Regional Effects of Condensation and Convection on δD

[15] Observations with higher relative humidity are more likely to have experienced recent condensation [*Cau et al.*, 2007], while observations with more negative lapse rates (less stable) indicates that the atmosphere is more likely to have undergone vertical mixing. In the latter case, evaporated moisture near the surface will have been lofted into the lower troposphere. Significant and negative linear regression coefficients for δD regressed against relative humidity are seen during the wet season of each region (Table 1), and are very similar in magnitude between regions. These coefficients suggest that local condensation is a significant driver of isotopic depletion, yet a second mechanism can also explain this result. Specifically, low-humidity conditions are more likely to drive strong evaporation of less depleted water from the surface, which would allow for increased vertical transport of less depleted moisture into the 500–825 hPa layer. The squares of multiple correlation values indicate that 30%, 14%, and 26% of the variance in wet season δD values is explained by the five predictors for the Amazon, Asian monsoon, and north Australian regions, respectively (Table 2). The explained variance in wet season δD values drops substantially to 9% for the Amazon and 4% for the Asian monsoon region when relative humidity is removed as a predictor in the multiple regression models. The partial correlations between δD and lapse rate are insignificant during these two regions' wet seasons, and further suggest that isotopic depletion by large-scale condensation is the dominant effect on isotopic variability (Table 2). Conversely, the explained variance in δD values over the Australian region is reduced to 20% when either the relative humidity or lapse rate predictors (both have negative regression coefficients) are removed from the five-variable, multiple regression model. This result supports a mechanism whereby surface evaporation and the vertical transport of less depleted boundary layer vapor influence the isotopic composition within the 500–825 hPa layer during dry conditions. Therefore, the multiple regression models suggest that condensation is the dominant control on isotopic variability during the wet seasons of the Amazon and Asian monsoon regions, but that convection and condensation are equally dominant during north Australia's wet season. These differences in regional hydrology are partially responsible for the DJF-JJA δD value difference between regions (Figure 2c).

[16] During the dry season, the Amazon shows a significant negative linear relationship between δD and RH (−0.13; Table 1), whereas the Australian and Asian monsoon regions show significant positive relationships (0.16 and 0.28, respectively). The Amazon dry season humidity at the 500–825 hPa level remains high (50–90% higher than the other regions), and the negative relationships between δD with RH and lapse rate may be explained by the mechanisms given for the north Australian wet season (above). For the drier Australian and Asian monsoon atmospheres, however, the entrainment of humid and isotopically heavy boundary layer air appears to increase both the δD values and the relative humidity in the 500–825 hPa layer, resulting in the positive linear regression coefficients witnessed in Table 1. Additionally, Table 1 indicates that the lowest dry season δD values occur during warm, dry, and stable conditions for these two regions, which suggests that subsidence plays a major role in supplying dry air to these regions and controls the most depleted isotopic values. However, the influences of advection affect the interpretation of the Asian monsoon and north Australian dry season hydrologic systems. This aspect will be thoroughly addressed in sections 3.3 and 4.

[17] Precipitation rates have been found to influence isotopic composition during the monsoonal seasons, and are suggested as one cause of the amount effect [e.g., *Matsuyama et al.*, 2005; *Vuille et al.*, 2005]. Table 1 shows significant negative relationships between wet season δD values and GPCP daily rainfall rates for all regions. At first glance, the fact that the strongest standardized linear correlation between δD and precipitation occurs over the drier north Australian region suggests that the kinetic isotopic effects of rainfall evaporation may be an important part of the amount effect. However, the partial correlations of δD versus precipitation are only significant for the Amazon wet season, where the explained variance in δD drops slightly to

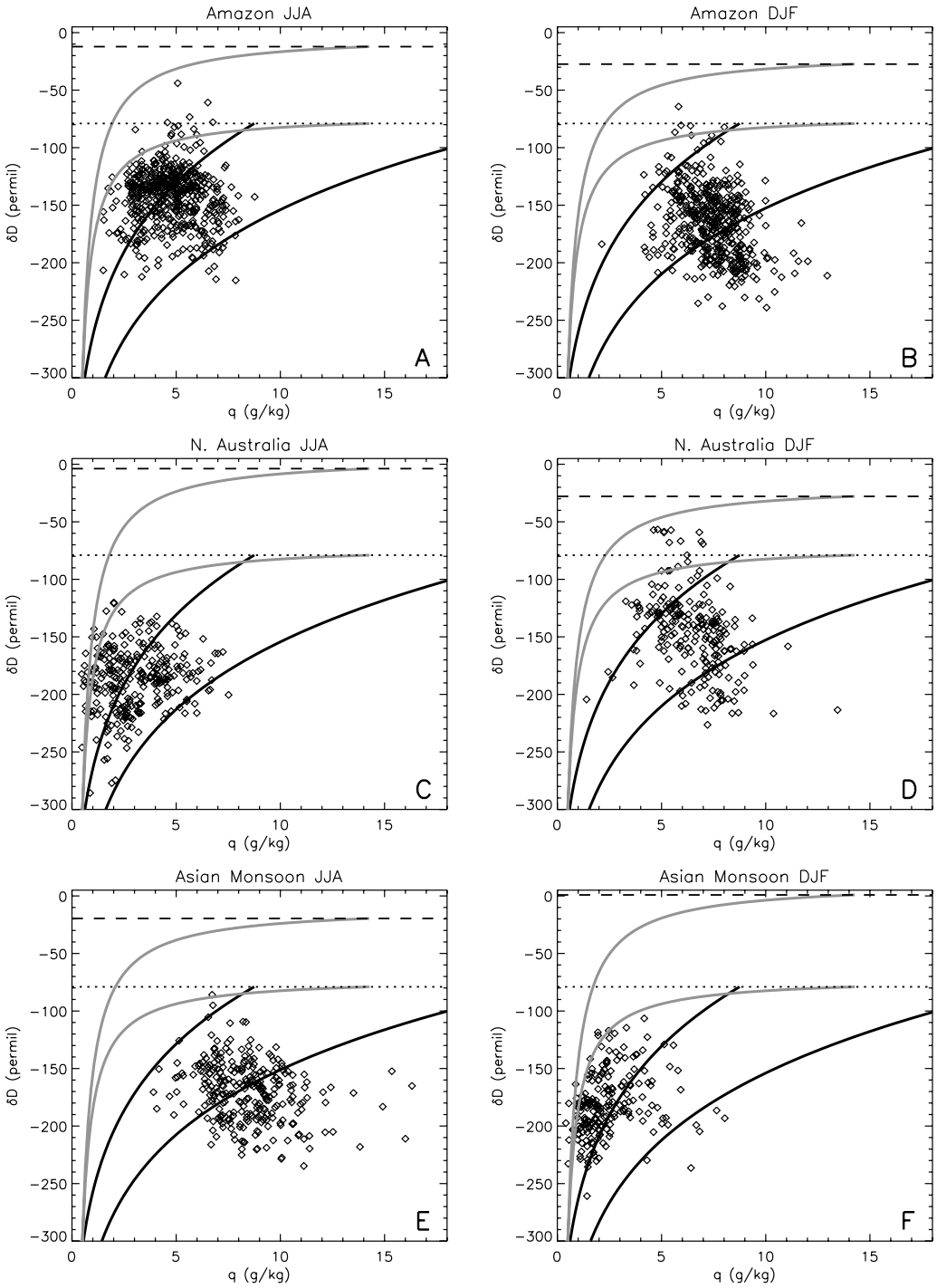

Figure 3. Regional δD as a function of specific humidity (q) for (a) Amazon JJA, (b) Amazon DJF, (c) north Australia JJA, (d) north Australia DJF, (e) Asian monsoon JJA, and (f) Asian monsoon DJF. Rayleigh distillation lines (black) initialized at common ocean/atmospheric surface layer δD values of −79‰ (black dotted line) with saturation specific humidity values based on surface temperatures of 285 K (left black line) and 300 K (right black line). An evaporation line (lower gray line) is also shown for reference, initialized from a value for vapor in equilibrium with ocean water (δD value of −79‰) and a saturation specific humidity value based on a surface temperature of 292.5 K. Average seasonal δD values in precipitation for each region (based on GNIP observations) are also shown (black dash), with mixing lines (upper gray lines) for saturation specific humidity values based on surface temperatures of 292.5 K to indicate the upper bound imposed by transpiration.

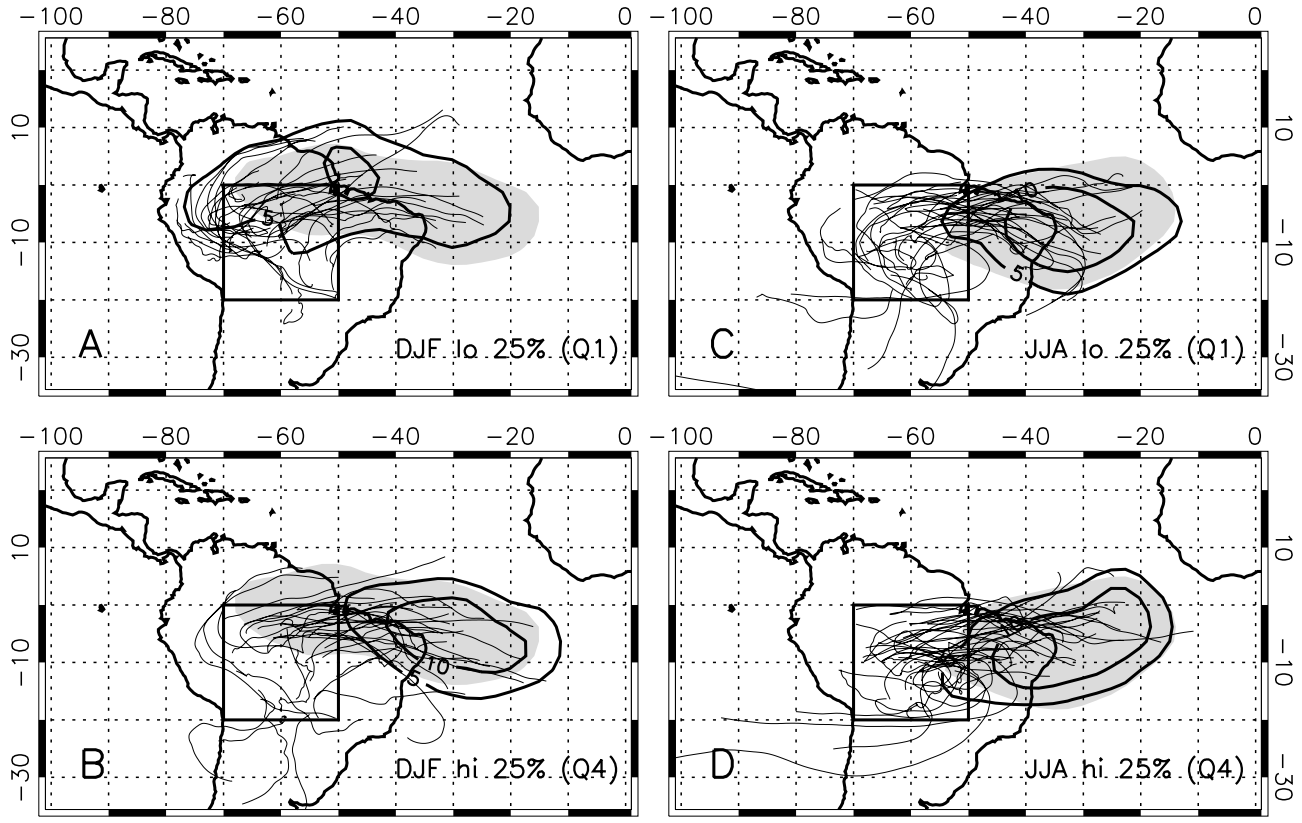

Figure 4. Probability distributions of 5-day trajectory origins for (a and b) DJF and (c and d) JJA for Q1 (Figures 4a and 4c) and Q4 (Figures 4b and 4d) δD from the Amazon region. Grey shading indicates 5%/10^6 km^2 of 5-day origins of DJF (JJA) δD values. Black contours indicate 5%/10^6 km^2 and 10%/10^6 km^2 of 5-day origins of Q1 (Q4) δD values. Each 10 by 10° box represents approximately 10^6 km^2. One in three Q1 (Q4) individual trajectory paths are shown in each case.

27% when precipitation is removed as a predictor (Table 2). The lowest δD values for the wet seasons of all regions (Figures 3b, 3d, and 3e) fall well below Rayleigh distillation predictions, yet the regression results indicate that with the exception of the Amazon region, the amount effect is acting upstream of the areas of interest during the monsoon seasons. The upstream aspect of the monsoonal hydrology will be addressed in section 4.

3.3. Regional Effects of Advection on δD

[18] When the atmosphere is unstable, turbulent mixing and convective transport can occur. If the local advection is strong, however, it will reduce the local signal of convective transport. Scalar moisture flux is used here as a measure of the rate at which the isotopic composition is changed by horizontal advection, and is similar to the advective rate parameter in the work of *Noone* [2008]. Scalar moisture flux can be considered related to the rate at which local isotopic values approach that of the upstream source. It is useful to note that advection can either enrich or deplete the regional isotopic composition because of the difference between the isotopic composition of the source and the local values. As such, advection differs from both condensation (which always depletes) and the influence of evaporated air from a local source (which usually enriches). Specifically, horizontal advection of depleted air parcels is linked to upwind condensation and hence fractionation, while advection of enriched vapor results if there has been little condensation en route from the evaporative source.

[19] Significant linear correlations between δD and scalar moisture flux values are seen for the north Australian and Asian monsoon wet seasons (−0.26 and −0.16, respectively; Table 1). However, the partial correlations between δD and scalar moisture flux values are statistically insignificant for these regions (Table 2) as a result of significant positive correlations between moisture flux and relative humidity (0.39 for north Australia and 0.28 for the Asian monsoon region). These relationships suggest that moisture advection acts to influence δD variability through its influence on humidity during the wet seasons of north Australian and Asian monsoon regions. Conversely, the significant and positive linear and partial correlations between δD and scalar moisture flux (Tables 1 and 2, respectively) indicate that strong moisture advection directly influences isotopic variability over the Amazon. However, these relationships also suggest that the lowest δD values, which are depleted beyond Rayleigh predictions, are observed primarily during relatively calm conditions. This association lends support to the argument that rainfall recycling that occurs locally over the Amazon basin acts to produce the anomalously low δD values during the wet season.

[20] The Asian monsoon dry season shows a positive linear correlation between δD and scalar moisture flux (0.27; Table 1), indicating that the horizontal advective

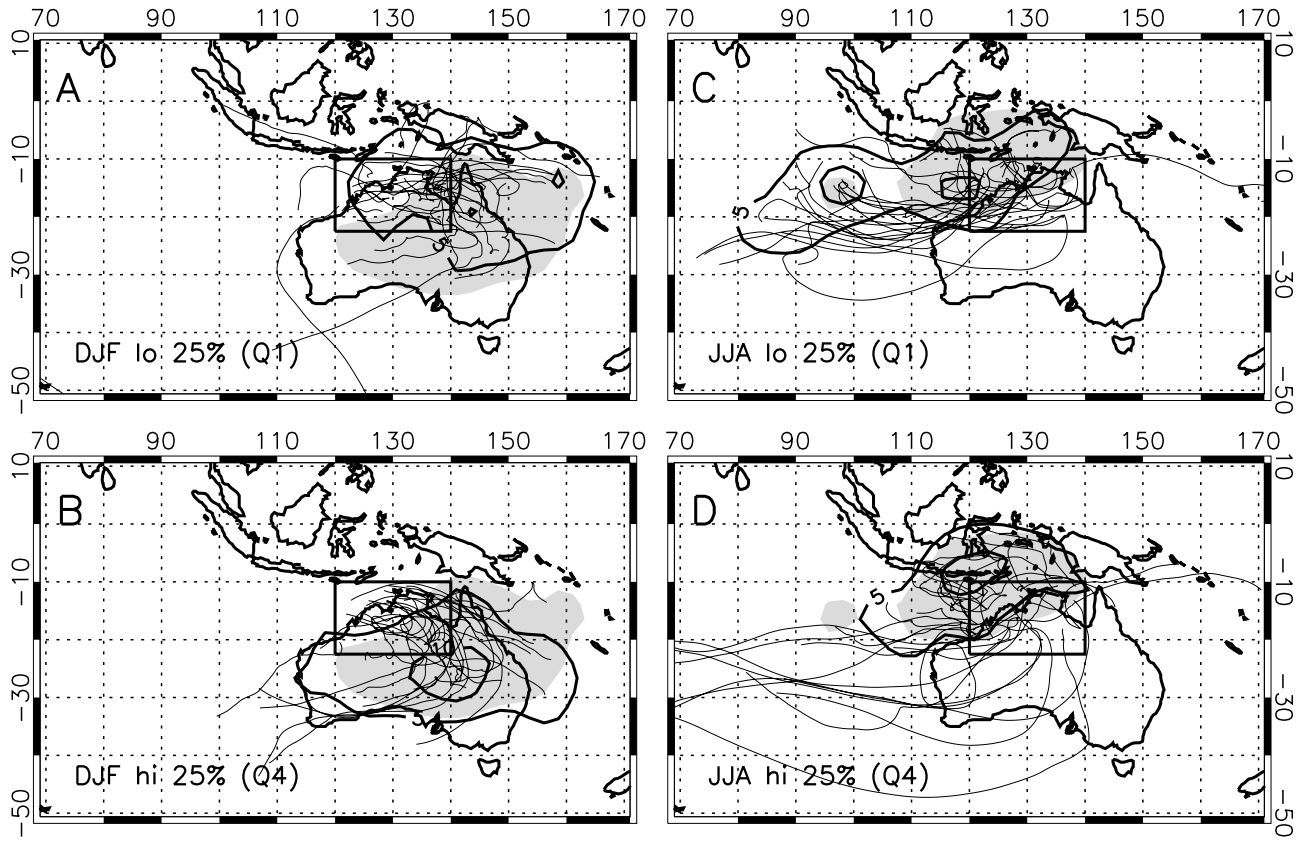

Figure 5. As in Figure 4 except for north Australian region. Trajectory plots from respective quartiles are overlaid from every second TES observation.

source is less depleted than the ambient air. The multiple regression analysis for this region shows that the lowest δD values occur during quiescent and warm synoptic conditions, which suggests that subsidence introduces the lowest δD values. The multiple regression model for the north Australian dry season suggests that the lowest δD values are largely associated with dry, stable, and windy conditions. It is clear that the stability of the overlying atmosphere dominates the isotopic variability of the 500–825 hPa layer during the north Australian dry season, since lapse rate associations control approximately half of the explained variance in δD values in the multiple regression model (Table 2). However, it remains unclear if the most depleted air parcels arrive from subsidence or via horizontal advection in this region. This uncertainty is addressed in more detail in section 4 using back trajectory analysis.

4. Hydrologic Balance of Tropical Continents

[21] Having established how various meteorological processes influence the isotopic composition of tropical continental areas, the task of assessing the regional hydrology of the three study regions with the TES HDO measurements is now tenable. Although the regression and correlation analyses described earlier are useful for gaining initial insight to the local controls on isotopic ratios, only a small percentage of the total variance in each region is captured by the local correlations alone (8–30%; Table 2, column 3). This result makes clear that the variance in isotopic composition of the remote water sources (both upstream and near-surface) associated with the long-range advection and the entrainment of lower-level vapor is important, and must be accounted for to fully explain the observed variance in the regional observations.

4.1. Difference in Seasonal Hydrology Across Regions

[22] A large component of seasonal hydrologic change is associated with changes in advective pathways. To quantify this, back trajectories originating from each TES observation location were calculated using three-dimensional wind fields from NCAR/NCEP Reanalysis data [*Kalnay et al.*, 1996], and assuming an arrival height of 670 hPa (in the middle of the 500–825 hPa layer). Vertical (“sigma”) velocity is estimated from the horizontal wind fields and surface pressure tendency through integration of the continuity equation to each of the 28 sigma levels in the Reanalysis data. The trajectory model uses tricubic interpolation in space and linear interpolation in time to find the wind at the trajectory locations [*Noone and Simmonds*, 1999]. Integration of the trajectory equation uses a fourth-order Runge-Kutta scheme and a time step of 20 min. The probability distributions of trajectory origins 5 days prior to the observations are shown in Figures 4–6a as the gray shaded region where the likelihood exceeds 5%/10^6km. Following the work of *Noone et al.* [1999], the probability distribution is computed by convolving the trajectory points with a Cressman-type weighting function with a mean radius of influence 500 km. The global integral of the probability density field is 100%, and the total seasonal percentage of parcel origins inside each the gray shaded

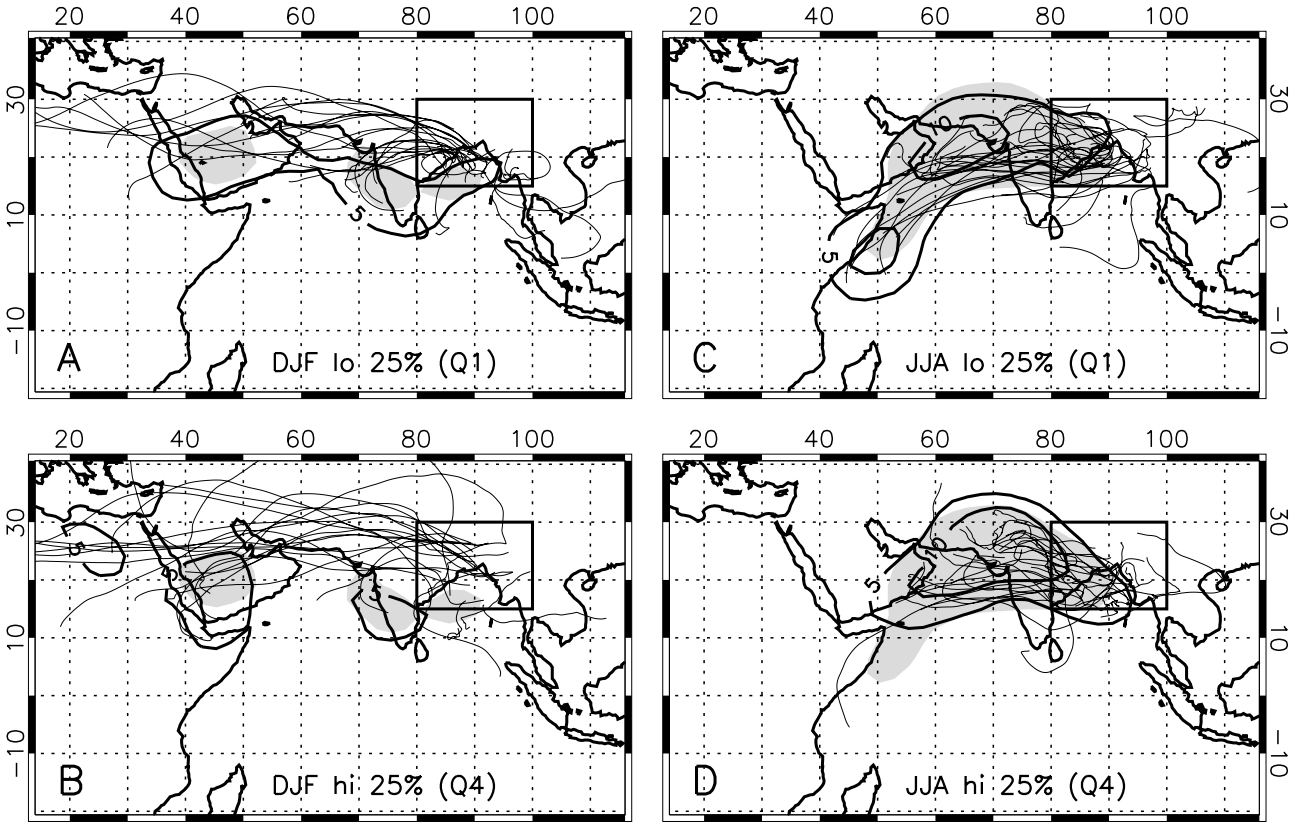

Figure 6. As in Figure 4 except for Asian monsoon region. Trajectory plots from respective quartiles are overlaid from every second TES observation.

regions in Figures 4–6 is approximately the number of 10° longitude by 10° latitude grid boxes within the contour times 5%. The solid contours in Figures 4–6 are for quartile analysis, and are discussed in section 4.2 (below).

[23] The origin probability distribution for the Amazon shows that the wet season (DJF; gray shading in Figures 4a and 4b) parcels tend to originate from further north than those of the dry season (JJA; Figures 4c and 4d). The wet season 5-day trajectories for the Asian monsoon (JJA; Figures 6c and 6d) and north Australian (DJF; Figures 5a and 5b) regions are generally less variable in origin locations and shorter in length than those during their dry seasons (Figures 6a and 6b and 5c and 5d, respectively), and are consistent with relatively steady monsoonal flow.

[24] Beyond this kinematic result, the δD frequency distributions for the DJF and JJA 5-day origin regions, as well as the frequency distributions at the observation sites, are shown in Figure 7. The frequency distributions of the origin regions are constructed for each season by taking all TES δD values within a 50 km radius of the positions of the 5-day back trajectories. The values are adjusted for altitude on the basis of the vertical change in δD found in individual TES δD profiles between 500 hPa and 825 hPa (typically 30‰/km, but different from profile to profile), and the change in height deduced from the trajectory calculation. This origin frequency distribution captures the variation in the seasonal mean distribution of values upstream of the respective regions. This is appropriate for the analysis as it is found in detailed examination of individual 5-day trajectories that the observed isotope signal is mostly set by moist processes that are associated with the monsoonal areas. This time frame also allows for an accurate diagnosis of large-scale subsidence. Thus, the difference in the distribution from the upstream origin to final observation provides the signature of exchange processes (or lack thereof), which can be understood in detail by considering the conditions experienced by the air parcels during transport.

[25] Along the trajectory path, specific humidity, temperature and geopotential height are found via interpolation from the Reanalysis grid to the three-dimensional trajectory point. For all regions, the wet season air parcels come from much lower in the atmospheric column than those of the dry season, and are generally associated with condensation during ascent (see section 4.2, below). This is evident in the frequency distributions of the origin and observation site δD values for DJF and JJA (Figure 7), which show that the 5-day origin mass weighted average δD values are less depleted during the wet season than those of the dry season. Very strong isotopic depletion en route during the wet season in the Amazon and Asian monsoon regions (a mean isotopic change of −40‰ and −44‰, respectively; Figures 7a and 7f) exceeds that from Rayleigh distillation expectations (−32‰ and −28‰, respectively), and can be explained by isotopic exchange during rainfall evaporation [e.g., *Worden et al.*, 2007]. The north Australian wet season exhibits no change in mean isotopic composition en route, although the shape of the frequency distribution changes substantially (DJF; Figure 7b). Further, it is evident that condensation is occurring in this region since many δD values are lower than Rayleigh distillation predictions (Figure 3d). Thus,

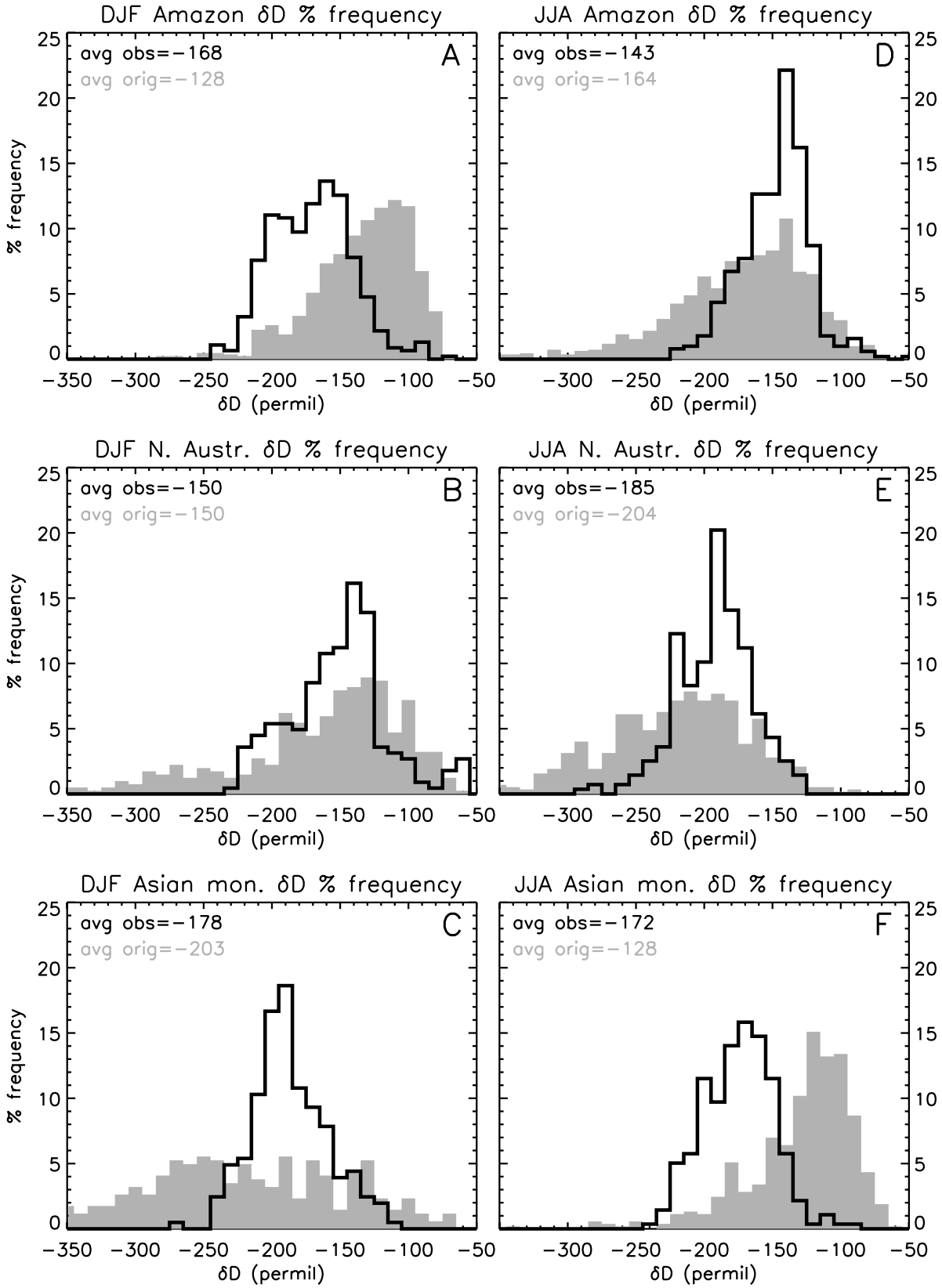

Figure 7. Frequency distribution of δD values over the layer 500–825 hPa for (a–c) DJF and (d–f) JJA seasons for the Amazon (Figures 7a and 7d), north Australian (Figures 7b and 7e), and Asian monsoon (Figures 7c and 7f) regions. Grey shading represents δD value distribution within the region close to the 5-day back trajectory origins, while black line represents the distribution within the regions.

Table 3. Mean δD and Standard Deviations for the Upper (Q4) and Lower (Q1) Quartiles of 5−Day Parcel Origin and Observation Site Locations[a]

			Mean δD		Stddev δD		$\Delta(\delta$D)
Region	Season	Quartile	Origin	Observation Site	Origin	Observation Site	Observation Site−Origin
Amazon	DJF	Q1	−127	−203	38	11	−76
Amazon		Q4	−130	−129	56	17	+1
Amazon	JJA	Q1	−153	−175	60	14	−22
Amazon		Q4	−176	−113	61	15	+63
North Australia	DJF	Q1	−151	−193	69	15	−42
North Australia		Q4	−161	−104	82	23	+57
North Australia	JJA	Q1	−207	−221	55	17	−14
North Australia		Q4	−203	−154	70	13	+51
Asian monsoon	DJF	Q1	−203	−214	66	13	−11
Asian monsoon		Q4	−198	−143	99	15	+55
Asian monsoon	JJA	Q1	−121	−204	32	11	−88
Asian monsoon		Q4	−141	−139	40	14	+2

[a]The change in δD from origin to site, $\Delta(\delta$D), is listed in column 8.

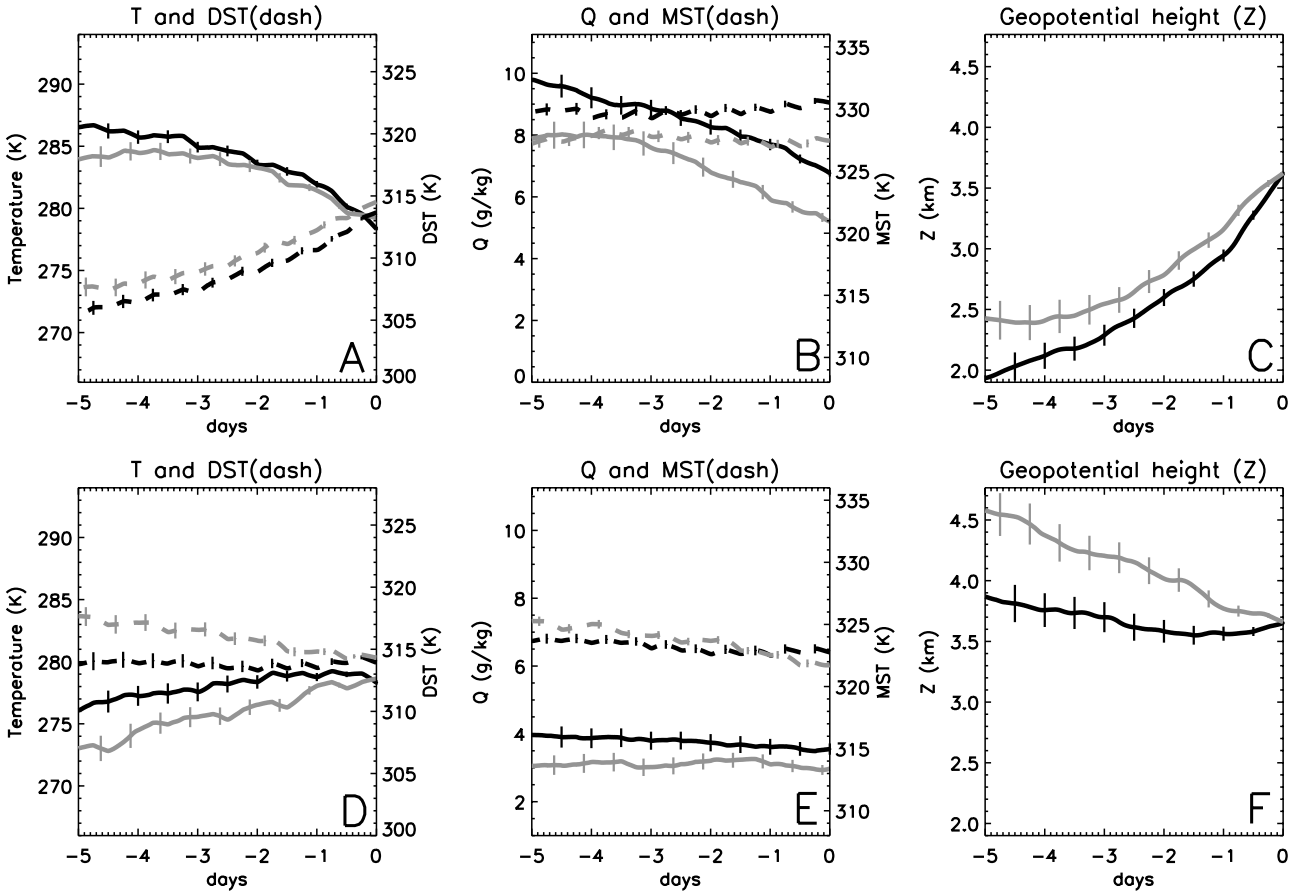

Figure 8. Amazon 5-day histories for (a−c) DJF and (d−f) JJA along computed trajectories of temperature and dry static temperature (dashed) (Figures 8a and 8d), specific humidity and moist static temperature (dashed) (Figures 8b and 8e), and geopotential height (Figures 8c and 8f). Black lines indicate the mean of Q1 air parcels, while gray lines indicate the mean of Q4 air parcels. In all plots and between each plot, the vertical axes are scaled such that vertical displacements in any panel are "energy conservative" and can be compared to the same vertical displacement in other panels. For example, changes of specific humidity or geopotential height scale exactly with the changes in temperature that MST or DST would experience from such change. Errors bars show the uncertainty (1σ) of the mean.

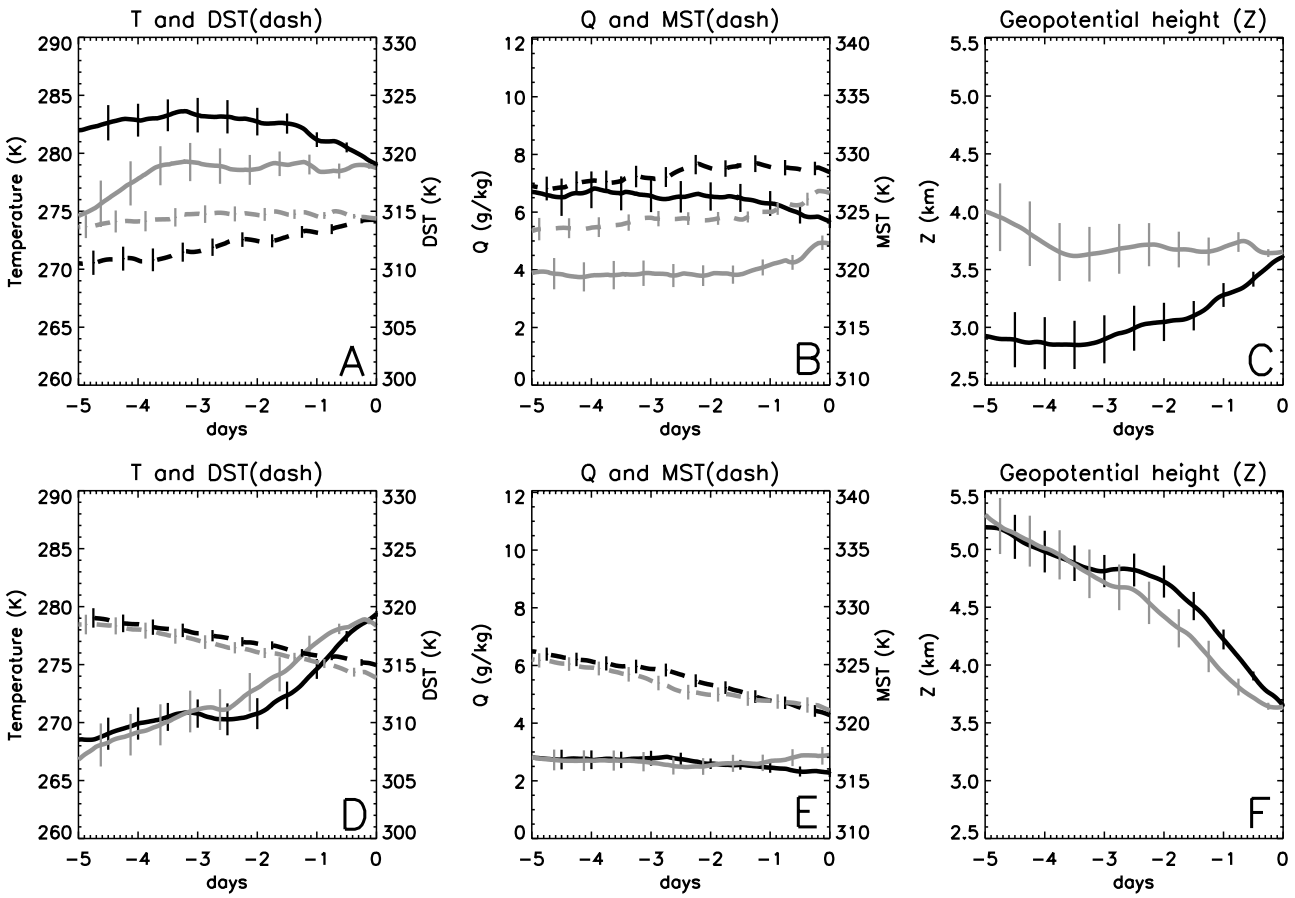

Figure 9. As in Figure 8 except for north Australian region.

rather than indicating that there is no hydrologic exchange along the trajectory paths, this apparent isotopic balance shows mixing with less depleted water from the near surface, which counteracts the isotopic depletion that results from condensation.

4.2. Processes Contributing to Intraseasonal Variability

[26] To illustrate the range of atmospheric processes contributing to the distribution of TES δD values, the δD observations in each region are partitioned into the most depleted (Q1) and least depleted (Q4) quartiles. In Figures 4–6, a subset of the 5-day trajectories within each quartile is shown in each panel (every third trajectory for the Amazon region, and every second trajectory for the north Australian and Asian monsoon regions). The moisture weighted mean and standard deviation of δD for the lowest (Q1) and highest (Q4) quartiles within both the 5-day origin and the final TES observation locations are given for each region in Table 3.

[27] To aid in assessing the roles of subsidence and condensation, dry and moist static energy are computed and are useful diagnostics because they are conserved during adiabatic and pseudoadiabatic processes, respectively [*Back and Bretherton*, 2006]. These quantities have been normalized by the specific heat of dry air at constant pressure (c_p), such that they have units comparable to potential temperature and equivalent potential temperature. Thus, the normalized variables, dry static temperature (DST) and moist static temperature (MST), are defined as

$$DST = T + \frac{g}{c_p} z \tag{3}$$

$$MST = DST + \frac{L}{c_p} q \tag{4}$$

where T is temperature, g is gravitational acceleration, z is geopotential height, q is specific humidity, and L is the latent heat of vaporization of water. The temperature, dry static temperature, specific humidity, moist static temperature, and geopotential height values within the parcels over the 5-day approach to the regions are shown in Figures 8–10. Note that the vertical axes of each panel in Figures 8–10 are scaled to have comparable units of energy such that a vertical displacement in one panel is the same vertical displacement on all others.

4.2.1. Wet Season Processes

[28] During the regional wet seasons, Q1 (most depleted) air parcels originate relatively closer to the equator (Figures 4a, 5a, and 6c) and lower in the atmosphere (Figures 8c, 9c, and 10f) 2than the Q4 (least depleted) air parcels in all cases. Additionally, the Q1 δD values for the wet seasons show isotopic depletion from the 5-day origins to observation

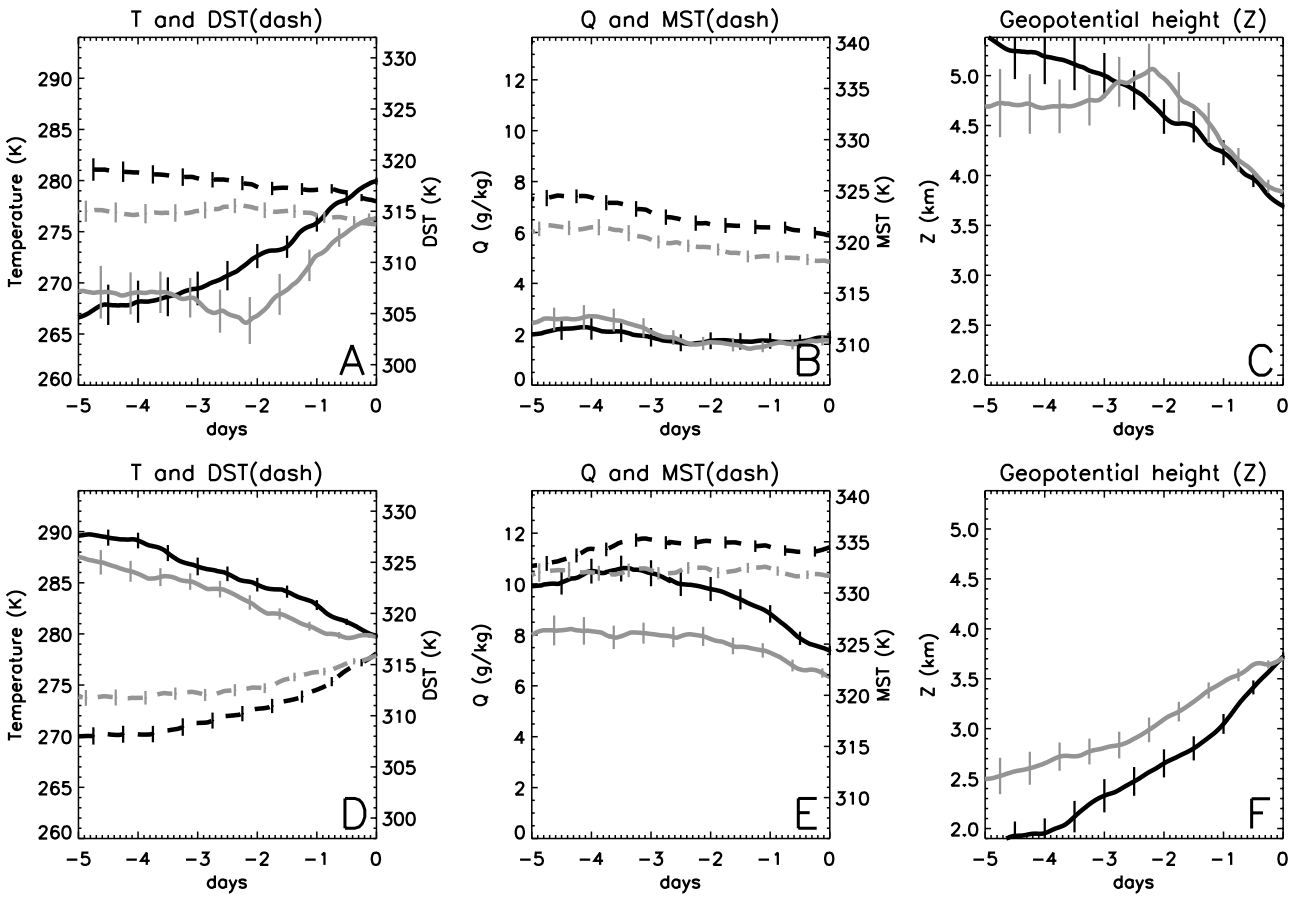

Figure 10. As in Figure 8 except for Asian monsoon region.

sites (δD difference of −76‰ for the Amazon, −42‰ for north Australia, and −88‰ for the Asian monsoon region; Table 3). Conditions within the relatively moist Q1 parcels indicate condensation en route via decreasing specific humidity values and generally constant MST values (Figures 8b, 9b, and 10e). Using these specific humidity values and the upstream δD values, Rayleigh distillation (equation (2)) consistently results in an underestimation of the observed depletion (−33‰ for the Amazon, −14‰ for north Australia, and −25‰ for the Asian monsoon region). This mismatch indicates isotopic exchange acting during strong condensation and rainfall during the monsoon season as shown by *Worden et al.* [2007].

[29] The wet season Q4 air parcels for the Amazon and Asian monsoon regions increase in geopotential height (Figures 8c and 10f), decrease in specific humidity, and maintain constant MST values (Figures 8b and 10e) en route. This supports condensation, and hence isotopic depletion (Rayleigh distillation predicts 37‰ and 20‰ depletion for the Amazon and Asian monsoon regions, respectively), yet there is almost no change in δD values across the 5-day path (Table 3). Recall that from above, the linear regression coefficients between δD with lapse rate and relative humidity suggest that local convective processes over the Amazon strongly influence the local hydrology (Table 1). The present results suggest that along the moisture pathway, a balance between the enrichment caused by supply from convective detrainment and the depletion caused by condensation leads, remarkably, to a nearly constant isotope ratio. Although qualitative in nature, this result illustrates the value of isotopes in identifying multiple exchange processes that can otherwise be overlooked if only the net change in observed moisture is considered.

[30] For the Asian monsoon region, the highest wet season δD values (i.e., Q4) primarily occur during quiescent times, as indicated by low scalar moisture flux (Table 1), and the associated air parcels are those which travel primarily over India (Figure 6d). These factors suggest a connection between the land surface and isotopic enrichment of the Q4 air parcels, since slowly moving air parcels have more opportunity to mix with air near the land surface. However, because of a lack of correlation between δD values and lapse rates, evidence for a specific mechanism for vertical transport of moisture into the 500–825 hPa layer (e.g., by convection or turbulent transport) cannot be identified. Similar to the Asian monsoon region, the north Australian wet season Q4 air parcels generally originate closer to the Australian continent and travel more slowly than the Q1 air parcels (Figure 5), allowing surface exchange to influence the parcel's isotopic composition (i.e., through convective detrainment). The wet season Q4 air parcel histories for north Australia do not indicate large-scale condensation, as shown by the increasing specific humidity and MST values over time (Figure 9b), and the lack of ascent to the observation locations (Figure 9c). These values show a 57‰ enrichment over the 5-day period

(Table 3), which is likely due to convective detrainment of relatively enriched and moist air plumes originating from the boundary layer, as shown by both the correlation between δD and lapse rate (Table 1) and by the increase in specific humidity along a constant trajectory height as the parcels approach the TES observation locations (Figure 9b).

[31] For all regions, the wet season Q4 δD values indicate moisture derived from the surface plays an important role for the regional hydrology. On the other hand, through enhanced isotopic depletion (i.e., greater than Rayleigh), the Q1 δD values indicate that rainfall reevaporation also plays a role. Similar processes (i.e., enhanced isotopic depletion through heavy rainfall and isotopic enrichment due to convective detrainment and turbulent transport) add to intraseasonal isotopic variability in all three regions. However, the effects of isotopic enrichment via convective detrainment are much greater during the wet season of north Australian than in those of the Amazon and Asian monsoon regions.

4.2.2. Dry Season Processes

[32] For the Amazon and north Australian regions, the histories of the dry season Q4 air parcels show steady specific humidity values (Figures 8e and 9e) and decreasing geopotential heights (Figures 8f and 9f). Additionally, the decreasing DST (Figures 8d and 9d) are consistent with radiative cooling (cooling of $\approx$ 1 K/d), and further indicate large-scale subsidence. For the Asian monsoon region, the Q4 trajectories show flow around the Himalayan Plateau 2 days prior to arrival (Figure 6b), followed by subsidence to the observation locations (as seen in Figures 10a–10c as decreasing DST values, steady specific humidity values, and decreasing altitude).

[33] The dry season Q4 air parcels arrive at the observation sites having become enriched relative to the mass weighted mean values of the source regions (63‰ enrichment for the Amazon, 51‰ for north Australia, and 55‰ for the Asian monsoon; Table 3). This observed isotopic enrichment of the Q4 air parcels is unexpected for large-scale subsidence, yet can be explained by a contribution from even modest, upward vertical transport of moist, less depleted air into the 500–825 hPa layer (consider the mostly vertical shape of the hyperbolic mixing lines at low specific humidity in Figure 3). This argument is supported by the significant and negative coefficients found in the linear regressions of δD and lapse rate (Table 1), which suggest an influence from convection or turbulent mixing. Put in this context, the positive correlations between δD and RH for the north Australian and Asian monsoon regions suggest that the mixing in of low-level moisture (through convective detrainment or turbulent transport) is a dominant process in controlling the (low) humidity in the regions. Conversely, because the Amazon dry season atmosphere is often closer to saturation than the other regions, the negative correlation between δD and RH (Table 1) suggests either that evapotranspiration is constrained by the humidity of the overlying atmosphere or that frequent condensation is a more dominant depleting effect for the local δD values.

[34] The dry season Q1 air parcels subside toward the TES observation sites over the north Australian and Asian monsoon regions, while the DST values decrease at a rate consistent with radiative cooling (around 1K/d; Figures 9d and 10a). The respective Q1 isotopic values change very little under these conditions (Table 3), and suggest that the lowest seasonal δD values act as a tracer of subsidence for these two regions. The linear correlations in Table 1 support this argument, where the lowest dry season δD values over north Australia and the Asian monsoon regions occur during warm, dry, and stable periods. For the Asian monsoon region, evidence for subsidence is provided by the positive correlation between δD and scalar moisture flux, which indicates that low δD values are associated with quiescent conditions. For north Australia, the trajectory lengths are generally shorter for the Q1 δD values than those of the Q4 values (compare Figures 5c and 5d), suggesting a similar relationship. Conversely, the Amazon dry season Q1 δD values show a depletion of 22‰ en route, while the associated air parcel histories support condensation via the steady MST values and slightly decreasing specific humidity values. Hence, variations in the degree of condensation during transport from the upstream origin, and variations in the limitation on local evapotranspiration due to high local humidity, are the primary drivers of intraseasonal dry season δD variability in this region.

[35] The dry season δD quartile analysis reveals that dry, subsiding air over the north Australian and Asian monsoon regions is a major part of the regional hydrology, but that occasional mixing with surface-derived moisture acts to partially control humidity in those regions. In contrast, while the Amazon region also experiences large-scale subsidence, powerful low-level convection acts to enrich all subsiding air parcels quickly. Additionally, the Amazon experiences condensation during the dry season, which is far stronger than during the dry season for the other two regions. Thus, the dry season Amazon hydrology is an involved mix of evaporative exchange and condensation, which is unique compared to the dry seasons of the north Australian and Asian monsoon regions. This complexity is not easily understood without isotopic constraints.

5. Conclusions

[36] Isotopic measurements from TES were used to examine the differences in the hydrology of three tropical continental areas. The TES data set used here spans 3 years and thus provides initial insight to the regional climatology. Some aspects of the balance of hydrologic processes can be resolved using TES isotopic data, and provides new opportunities for understanding the movement of water in the climate system. To do so with confidence, the factors controlling the isotopic signals over three geographically different, yet convectively active, continental regions were established. Important regional differences in hydrology emerged by comparison of the dominant seasonal and intraseasonal controls on mean δD values.

[37] Results show differences in the seasonal controls (condensation, convection, and subsidence) on the δD values lead to the regional differences in DJF-JJA δD values (recall Figure 2c). The isotopic depletion caused by intense condensation in the Asian monsoon wet season is strong enough to cause δD values approximately equal to those of the subsidence-controlled dry season. For the Amazon, intense condensation produces much lower δD values than does intermittent condensation and convection during the dry season. During the wet season, variations in the strength

of monsoonal condensation and boundary layer ventilation events introduce variability in north Australian δD values, however the DJF-JJA δD difference appears to be dominated by the intrusion of isotopically depleted vapor during dry season subsidence.

[38] The lowest δD values observed during all regional wet seasons show isotopic depletion beyond that predicted by Rayleigh distillation. This indicates an "amount effect" on vapor phase stable water isotopes, and that in-cloud isotopic exchange and rainfall evaporation are an important part of the regional hydrologic budget. The study by *Vimeux et al.* [2005] found no relationship between isotopic values in precipitation with local temperature or local rainfall rates near Bolivia. While the present study also finds no significant correlations between δD values and temperature during the regional monsoons, it does show that rainfall rates affect the δD values of tropospheric water vapor over the Amazon. Thus, this study incorporates and extends the findings of *Rozanski et al.* [1993] and *Worden et al.* [2007], by showing that the amount effect primarily occurs upstream of monsoonal regions, but that it also occurs within the regional boundaries of the Amazon.

[39] Results confirm that while Rayleigh distillation is useful in explaining some features in the regional δD values, additional isotopic exchange during heavy monsoonal rainfall and turbulent transport of boundary layer moisture makes the δD distributions over monsoonal areas highly non-Rayleigh in nature. Relatively high δD values during times of weaker stability, as measured by the lapse rate, show that local convection is important for the near surface hydrology of monsoonal regions. The balance between convective moisture transport and the condensation in the region of convection is important for the local surface latent heat budget. Similar results that indicate the importance of convective moisture transport were found in the region of convective clouds in models by *Schmidt et al.* [2005] and from aircraft observations by *Webster and Heymsfield* [2003]. In the present study, the local convective effect is most pronounced over both the dry and wet season of north Australia, as well as during the dry season of the Amazon. Anomalously high dry season δD values over the Amazon indicate that convection transports boundary layer moisture into the overlying atmosphere [e.g., *Worden et al.*, 2007], which is likely partially composed of transpired water. This result is in general agreement with the work of *Henderson-Sellers et al.* [2002].

[40] Future work to estimate the degree of rainfall evaporation and supply of boundary layer air in these regions must incorporate knowledge of the boundary layer δD values. Since the TES instrument is primarily sensitive to H_2O and HDO above the height of the boundary layer (maximum sensitivity is 500–825 hPa), the boundary layer values must be inferred from modeling or from surface measurements of vapor or precipitation. To this end, direct measurement of the isotopic composition of low-level vapor would aid in resolving the amount of continental water recycling which occurs over each region. However, by combining information about standing water, soil and vegetation properties with observed δD values of precipitation, the isotopic composition of moisture from surface fluxes can be inferred, and used to constrain an adequate hydrologic exchange model. The success of the present study, which focuses on process analysis, gives confidence that more sophisticated modeling and assimilation approaches can be used in conjunction with the TES HDO data to assess the global and regional scale hydrology.

[41] **Acknowledgments.** The authors would like to thank Manvendra Dubey at Los Alamos National Laboratory for his encouragement of this work and Kevin Bowman at NASA's Jet Propulsion Laboratory for assisting with development of the TES HDO product. Support for this study came from a Graduate Research Environmental Fellowship from the U.S. Department of Energy's Office of Biological and Environmental Research and funding from the Jet Propulsion Laboratory. A portion of the research described in this paper was carried out at the Jet Propulsion Laboratory, California Institute of Technology, under a contract with the National Aeronautics and Space Administration.

References

Araguas-Araguas, L., K. Froehlich, and K. Rozanski (1998), Stable isotope composition of precipitation over southeast Asia, *J. Geophys. Res.*, *103*(D22), 28,721–28,742, doi:10.1029/98JD02582.

Araguas-Araguas, L., K. Froehlich, and K. Rozanski (2000), Deuterium and oxygen-18 isotope composition of precipitation and atmospheric moisture, *Hydrol. Processes*, *14*, 1341–1355, doi:10.1002/1099-1085(20000615)14:8<1341::AID-HYP983>3.0.CO;2-Z.

Back, L. E., and C. S. Bretherton (2006), Geographic variability in the export of moist static energy and vertical motion profiles in the tropical Pacific, *Geophys. Res. Lett.*, *33*, L17810, doi:10.1029/2006GL026672.

Blunier, T., J. Schwander, J. Chappellaz, F. Parrenin, and J. M. Barnola (2004), What was the surface temperature in central Antarctica during the last glacial maximum?, *Earth Planet. Sci. Lett.*, *218*(3–4), 379–388, doi:10.1016/S0012-821X(03)00672-1.

Cau, P., J. Methven, and B. J. Hoskins (2007), Origins of dry air in the tropics and subtropics, *J. Clim.*, *20*, 2745–2759, doi:10.1175/JCLI4176.1.

Dansgaard, W. (1964), Stable isotopes in precipitation, *Tellus*, *16*, 436–468.

Dirmeyer, P. A., R. D. Koster, and Z. Guo (2006), Do global models properly represent the feedback between land and atmosphere?, *J. Hydrometeorol.*, *7*, 1177–1198, doi:10.1175/JHM532.1.

Fricke, H., and S. L. Wing (2004), Oxygen isotope and paleobotanical estimates of temperature and δ^{18}O–latitudinal gradients over North America during the early Eocene, *Am. J. Sci.*, *304*, 612–635, doi:10.2475/ajs.304.7.612.

Fu, R., and W. Li (2004), The influence of the land surface on the transition from dry to wet season in Amazonia, *Theor. Appl. Climatol.*, *78*(1–3), 97–110, doi:10.1007/s00704-004-0046-7.

Gat, J. R. (1996), Oxygen and hydrogen isotopes in the hydrologic cycle, *Annu. Rev. Earth Planet. Sci.*, *24*, 225–262, doi:10.1146/annurev.earth.24.1.225.

Grootes, P. M., M. Stuiver, L. G. Thompson, and E. M. Thompson (1989), Oxygen isotope changes in tropical ice, Quelccaya, Peru, *J. Geophys. Res.*, *94*(D1), 1187–1194, doi:10.1029/JD094iD01p01187.

Henderson-Sellers, A., K. McGuffie, and H. Zhang (2002), Stable isotopes as validation tools for global climate model predictions of the impact of Amazonian deforestation, *J. Clim.*, *15*, 2664–2677, doi:10.1175/1520-0442(2002)015<2664:SIAVTF>2.0.CO;2.

Henderson-Sellers, A., K. McGuffie, D. Noone, and P. Irannejad (2004), Using stable water isotopes to evaluate basin-scale simulations of surface water budgets, *J. Hydrometeorol.*, *5*, 805–822, doi:10.1175/1525-7541(2004)005<0805:USWITE>2.0.CO;2.

Hoffmann, G. (2003), Taking the pulse of the tropical water cycle, *Science*, *301*, 776–777, doi:10.1126/science.1085066.

Jouzel, J., F. Vimeux, N. Caillon, G. Delaygue, G. Hoffmann, V. Masson-Delmotte, and F. Parrenin (2003), Magnitude of isotope/temperature scaling for interpretation of central Antarctic ice cores, *J. Geophys. Res.*, *108*(D12), 4361, doi:10.1029/2002JD002677.

Juárez, R. I. N., M. G. Hodnett, R. Fu, M. L. Goulden, and C. von Randow (2007), Control of Dry season evapotranspiration over the Amazonian forest as inferred from observations at a southern Amazon forest site, *J. Clim.*, *20*, 2827–2839, doi:10.1175/JCLI4184.1.

Kalnay, E., et al. (1996), The NCEP/NCAR 40-year reanalysis project, *Bull. Am. Meteorol. Soc.*, *77*, 437–471, doi:10.1175/1520-0477(1996)077<0437:TNYRP>2.0.CO;2.

Lawrence, J. R., S. D. Gedzelman, D. Dexheimer, H.-K. Cho, G. D. Carrie, R. Gasparini, C. R. Anderson, K. P. Bowman, and M. I. Biggerstaff (2004), Stable isotopic composition of water vapor in the tropics, *J. Geophys. Res.*, *109*, D06115, doi:10.1029/2003JD004046.

Malhi, Y., E. Pegoraro, A. D. Nobre, M. G. P. Pereira, J. Grace, A. D. Culf, and R. Clement (2002), Energy and water dynamics of a central Ama-

zonian rain forest, *J. Geophys. Res.*, *107*(D20), 8061, doi:10.1029/2001JD000623.

Martinelli, L. A., R. L. Victoria, L. S. Lobo Sternberg, A. Ribeiro, and M. Zacharias Moreira (1996), Using stable isotopes to determine sources of evaporated water to the atmosphere in the Amazon Basin, *J. Hydrol. Amsterdam*, *183*(3–4), 191–204, doi:10.1016/0022-1694(95)02974-5.

Matsuyama, H., K. Miyaoka, and K. Masuda (2005), Year-to-year variations of the stable isotopes in precipitation in February at Cuiab'a, located on the northern fringe of Pantanal, Brazil, *J. Hydrometeorol.*, *6*, 324–329, doi:10.1175/JHM419.1.

McGuffie, K., and A. Henderson-Sellers (2004), Stable water isotope characterization of human and natural impacts on land-atmosphere exchanges in the Amazon Basin, *J. Geophys. Res.*, *109*, D17104, doi:10.1029/2003JD004388.

Noone, D. (2008), The influence of midlatitude and tropical overturning circulation on the isotopic composition of atmospheric water vapor and Antarctic precipitation, *J. Geophys. Res.*, *113*, D04102, doi:10.1029/2007JD008892.

Noone, D., and I. Simmonds (1999), A three-dimensional spherical trajectory algorithm, in *Research Activities in Atmospheric and Oceanic Modelling, Rep. 28, WMO/TD-No. 942*, edited by H. Ritchie, pp. 3.26–3.27, World Meteorol. Organ., Geneva, Switzerland.

Noone, D., J. Turner, and R. Mulvaney (1999), Atmospheric signals and characteristics of accumulation in Dronning Maud Land, Antarctica, *J. Geophys. Res.*, *104*(D16), 19,191–19,212, doi:10.1029/1999JD900376.

Rozanski, K., and L. Araguas-Araguas (1995), Spatial and temporal variability of stable isotope composition of precipitation over the South American continent, *Bull. Inst. Fr. Etud. Andines*, *24*, 379–390.

Rozanski, K., L. Araguas-Araguas, and R. Gonfiantini (1992), Relation between long-term trends in oxygen-18 isotopic composition of precipitation and climate, *Science*, *258*, 981–985, doi:10.1126/science.258.5084.981.

Rozanski, K., L. Araguas-Araguas, and R. Gonfiantini (1993), Isotopic patterns in modern global precipitation, in *Climate Change in Continental Isotopic Records, Geophys. Monogr. Ser.*, vol. 78, edited by P. K. Swart et al., pp. 1–37, AGU, Washington, D. C.

Salati, E., and P. B. Vose (1984), Amazon Basin: A system in equilibrium, *Science*, *225*(4658), 129–138, doi:10.1126/science.225.4658.129.

Schmidt, G. A., G. Hoffmann, D. T. Shindell, and Y. Hu (2005), Modelling atmospheric stable water isotopes and the potential for constraining cloud processes and stratosphere-troposphere water exchange, *J. Geophys. Res.*, *110*, D21314, doi:10.1029/2005JD005790.

Sengupta, S., and A. Sarkar (2006), Stable isotope evidence of dual (Arabian Sea and Bay of Bengal) vapor sources in monsoonal precipitation over north India, *Earth Planet. Sci. Lett.*, *250*, 511–521, doi:10.1016/j.epsl.2006.08.011.

Tian, L., T. Yao, K. MacClune, J. W. C. White, A. Schilla, B. Vaughn, R. Vachon, and K. Ichiyanagi (2007), Stable isotopic variations in west China: A consideration of moisture sources, *J. Geophys. Res.*, *112*, D10112, doi:10.1029/2006JD007718.

Vimeux, F., R. Gallaire, S. Bony, G. Hoffman, and J. C. H. Chiang (2005), What are the climate controls on δD in precipitation in the Zongo Valley (Bolivia)? Implications for the Illimani ice core interpretation, *Earth Planet. Sci. Lett.*, *240*, 205–220, doi:10.1016/j.epsl.2005.09.031.

Vuille, M., M. Werner, R. S. Bradley, and F. Keimig (2005), Stable isotopes in precipitation in the Asian monsoon region, *J. Geophys. Res.*, *110*, D23108, doi:10.1029/2005JD006022.

Webster, C., and A. Heymsfield (2003), Water isotope ratios D/H, $^{18}O/^{16}O$, $^{17}O/^{16}O$ in and out of clouds map dehydration pathways, *Science*, *302*, 1742–1745, doi:10.1126/science.1089496.

Worden, J., et al. (2006), Tropospheric Emission Spectrometer observations of the tropospheric HDO/H_2O ratio: Estimation approach and characterization, *J. Geophys. Res.*, *111*, D16309, doi:10.1029/2005JD006606.

Worden, J., D. Noone, K. Bowman, R. Beer, A. Eldering, B. Fisher, M. Gunson, A. Goldman, R. Herman, and S. Kulawik (2007), Importance of rain evaporation and continental convection in the tropical water cycle, *Nature*, *445*(7127), 528–532, doi:10.1038/nature05508.

Wushiki, H. (1977), Deuterium content in the Himalayan precipitation at Khumbu District, observed in 1974/1975, in *Glaciers and Climates of Nepal Himalayas. Report of the Glaciological Expedition to Nepal: Part 2*, edited by K. Higuchi, C. Hakajima, and K. Kusunoki, *Seppyo*, *39*, 50–56.

D. Brown and D. Noone, Cooperative Institute for Research in Environmental Sciences, Campus Box 216, University of Colorado, Boulder, CO 80309-0216, USA. (derek.brown@colorado.edu)

J. Worden, Jet Propulsion Laboratory, California Institute of Technology, Pasadena, CA 91109, USA.